Atmospheric methane control mechanisms during the early Holocene

Ji-Woong Yang[1], Jinho Ahn[1], Edward J. Brook[2], and Yeongjun Ryu[1]

[1]School of Earth and Environmental Sciences, Seoul National University, Seoul 08826, South Korea

[2]College of Earth, Ocean, and Atmospheric Sciences, Oregon State University, Corvallis, OR 97331, USA

Correspondence to: Jinho Ahn (jinhoahn@snu.ac.kr)

Abstract. Understanding processes controlling atmospheric methane (CH_4) mixing ratio is crucial to predict and mitigate the future climate change. In spite of recent studies using various approaches for the last ~1000 to 2000 years, control mechanisms of CH_4 still remain unclear, partly because the late Holocene CH_4 budget is comprised of natural and anthropogenic emissions. In contrast, the early Holocene was a period when human influence should have been substantially smaller, so that it allows us to elucidate the natural controls under interglacial conditions. Here we present new high resolution CH_4 records from Siple Dome, Antarctica, covering from 11.6 to 7.7 thousands of years before 1950 AD (ka). We observe several local CH_4 minima on a roughly 1000-year spacing, which correspond to cool periods in Greenland. We hypothesize that the cooling in Greenland forced the Intertropical Convergence Zone (ITCZ) to migrate southward, reducing rainfall in northern tropical wetlands although there is no obvious change was observed in low latitude hydrology corresponding to abrupt CH_4 reduction at ~10.3 ka. Inter-polar difference (IPD) of CH_4 shows a gradual increase from the onset of the Holocene to ~9.9 ka, which implies growth of boreal source strength following the climate waring in the northern extratropics during that period. Finally, we find that amplitude of centennial- to millennial scale CH_4 variability of the early Holocene is larger on average than that of the earlier part of the late Holocene (3.5 – 1.2 ka).

1 Introduction

Methane (CH_4) is a potent greenhouse gas whose atmospheric mixing ratio has increased more than 2.5 times since the Industrial Revolution (Dlugokencky et al., 2009). Although lower in abundance compared to carbon dioxide (CO_2), CH_4 has ~28 times higher global warming potential (GWP) on centennial timescales, and even higher GWP on shorter time scales due to the shorter lifetime in the atmosphere (Stocker et al., 2013). Hence the knowledge of control mechanisms of CH_4 is important to predict and mitigate the future climatic and environmental changes.

Naturally, CH_4 is mainly produced by microbial decomposition by methanogens in anaerobic environments, such as waterlogged soil, wetlands, or sediments of lakes and rivers. Even though CH_4 can be oxidized and emitted as CO_2, a considerable amount of CH_4 is still released into the atmosphere through vascular plants, diffusion and ebullition processes (e.g., Joabsson and Christensen, 2001). Geological CH_4 released from mud volcanoes and gas seepages through faults is the

second most important natural source (e.g., Etiope et al., 2008 and references therein). Additionally, a portion of CH_4 is produced by termites and wild animals via microbial digestive process (e.g., Sanderson, 1996), and by pyrogenic sources such as wildfire and biomass burning (e.g., Andreae and Merlet, 2001; Ferretti et al., 2005; Hao and Ward, 1993). The oceanic CH_4 flux is considered as too small to create a significant change in global budget compared to the other sources (Rhee et al., 2009). The major sink of atmospheric CH_4 is photochemical reactions (oxidation) with the hydroxyl radical (OH), which is mainly controlled by atmospheric temperature, humidity, and mixing ratio of non-methane volatile organic compound (NMVOC) (e.g., Levine et al., 2011 and references therein). The air temperature affects air humidity, limiting the production of OH. Both NMVOCs and CH_4 are competing for OH to be oxidized, that is, increase in NMVOC emission reduces the available OH, so it increases the lifetime of CH_4 in the atmosphere (Valdes et al., 2005). Further, since the OH is produced by photo-dissociation reaction, the CH_4 sink strength is affected by light availability and tropospheric ozone (e.g., Levy, 1971). Polar winters may affect the CH_4 sink strength by reduced OH production rate, but the seasonal-scale cycles are not resolvable in ice core records due to gas dispersion in firn layers. However, recent model studies suggested the dominant role of source changes rather than sink in controlling atmospheric CH_4 during the past climate changes (Weber et al., 2010; Levine et al., 2011). Therefore, the sink changes are not considered here.

Since the direct CH_4 monitoring of modern air samples only covers the late 20^{th} and early 21^{st} centuries (Dlugokencky et al., 1994, 2011), investigation further back in time requires the unique archive of polar ice that preserves the ancient atmospheric air. Paleoatmospheric CH_4 levels have been reconstructed for the last 800 ka from Antarctic- and Greenland ice cores. Given the relatively long lifetime in troposphere (11.2 ± 1.3 years at present, e.g., Prather et al., 2012) compared to atmospheric mixing time, ice core CH_4 records represent well-mixed global signatures. From the 800 ka records, it was revealed that the past CH_4 change generally followed the glacial-interglacial cycles, being low during glacial periods and high in interglacials, as well as the shorter orbital cycles of obliquity and precession (e.g., Spahni et al., 2005; Loulergue et al., 2008). Those earlier studies have suggested that the changes in climate and hydrology on tropical wetlands induced by the orbital changes controlled the CH_4 emissions. The resemblance between water stable isotopes from Greenland ice cores, a proxy for Greenland climate change, and global CH_4 mixing ratio has been largely reported. This implies that local temperature change around Greenland could affect the major CH_4 sources in low latitudes (e.g., Brook et al., 1996; Chappellaz et al., 1993; Huber et al., 2006). The similarity is also held in short time scale climate events. Previous works reported that rapid CH_4 increases were coincident with abrupt climate changes in Dansgaard-Oeschger (DO) events during the glacial period (e.g., Brook et al., 1996; EPICA Community Members, 2006; Grachev et al., 2007, 2009). The coincidence between abrupt CH_4 and Greenland climate change was also found in 8.2k cooling event, Preboreal Oscillation (PBO), Younger Drays (YD), and Bølling-Allerød (BA) periods (Brook et al., 2000; Kobashi et al., 2007, 2008).

Intensive precipitation changes on the low latitude summer monsoon area by insolation changes (e.g., Asian monsoon) have been suggested as an important control during the glacial period (e.g., Chappellaz et al., 1990). From time series analysis of past CH_4 records, Guo et al. (2012) found that the tropical monsoon circulations are primary control of relatively shorter (millennial) time scale variability, while long-term (multi-millennial to orbital scale) variations are dominated by solar

insolation changes. It has been found that tropical monsoon activities were closely related to orbital-scale CH_4 change (e.g., Brook et al., 1996; Chappellaz et al., 1990), especially reported are Asian monsoon (e.g., Loulergue et al., 2008) and South American monsoon (e.g., Cruz et al., 2005). However, no direct correlation between CH_4 and tropical monsoon signals has been reported for the early Holocene, although demonstrated were the positive relationships between Greenland climate and tropical monsoons (e.g., Chiang et al., 2008), and between Greenland climate and CH_4 (e.g., Spahni et al., 2005; Wang et al., 2005; Mitchell et al., 2011) have been discussed. Given that waterlogged wetlands are the largest natural CH_4 source, this complex relationship may imply that tropical monsoons are not the sole, primary controls; wetlands in northern high latitude and southern hemisphere might act as a secondary role.

Relationship between the latitudinal shift of ITCZ and CH_4 emission varies with time scales. Landais et al. (2010) and Guo et al. (2012) suggested that ITCZ migration is not a dominant control of glacial-interglacial CH_4 cycle because long-term CH_4 trend does not follow well the precessional insolation change in the northern hemisphere. Modelling studies found the southward shift of ITCZ coincides with reduced CH_4 in Last Glacial Maximum (LGM) and Heinrich Stadial (HS) events, but changes in wetland area and surface hydrology were small (Weber et al., 2010; Hopcroft et al., 2011). They instead suggested that changes in temperature and/or plant productivity affected CH_4 production during those events. Rather, ITCZ migration appears to be related with millennial- or sub-millennial scale CH_4 change. Brook et al. (2000) found that submillennial-scale CH_4 minima during the last deglacial period correspond with reduced precipitation recorded in Cariaco Basin sediment data, which indicates southward displacement of ITCZ (Hughen et al., 1996). It is supported by spectral analysis of CH_4 during the past 800 ka record that found that ITCZ change becomes an important driver of millennial scale CH_4 change (Tzedakis et al., 2009; Guo et al., 2012).

The ice core scientists started to apply high-resolution CH_4 mixing ratio and stable isotope data to discern governing mechanisms of Holocene CH_4 variation, but currently the high-resolution records cover a part of the Holocene. High-resolution CH_4 records from Law Dome and WAIS Divide ice cores (Antarctica) show characteristic variability in multi-decadal to centennial time scale, apart from long-term gradual increasing trend (MacFarling-Meure et al., 2006; Mitchell et al., 2011). The high-resolution records were compared with various temperature- and precipitation proxies, but the previous works found no strong correlations that explain the observed decadal- to centennial scale variabilities. Limitation was that the late Holocene CH_4 budget may have been comprised of both natural and anthropogenic terms, making it difficult to distinguish between them. Mitchell et al. (2011) pointed out that some of abrupt CH_4 decreases could have resulted by historical events, such as Mongolian invasion, Plagues, or Spanish invasion. Later, Mitchell et al. (2013) made simultaneous measurement of Antarctic (WAIS Divide) and Greenland (GISP2) ices to derive IPD, and extended their high-resolution records back to ~4 ka. They used eight-box atmospheric methane model (EBAMM) and anthropogenic- and natural emission scenarios to investigate CH_4 control factors. Their results showed that the late Holocene CH_4 evolution can be explained by a combination of natural- and anthropogenic emissions. In the other hand, stable isotope ratios of CH_4 help us to distinguish the types of sources – biogenic, pyrogenic, and geologic. Sowers (2010) reconstructed CH_4 mixing ratio and stable isotope ratio of CH_4 ($\delta^{13}C$-CH_4 and δD-CH_4) throughout the entire Holocene and suggested several possible control factors, such as boreal wetlands and thermokarst

lakes, changing C_3/C_4 plant ratio of CH_4-emitting ecosystems, and changing composition of methanogenic communities. However, temporal resolution of the data (~138 years in average during 7.0 – 11.3 ka) was not sufficient to capture sub-millennial scale variability. Former studies have shown the reduction of pyrogenic emission and increased agricultural emission during the last millennia (Ferretti et al., 2005; Mischler et al., 2009). In later work using $\delta^{13}C$-CH_4 records from NEEM ice core, Sapart et al. (2012) found that the centennial-scale variations during the last two millennia were caused by changes in pyrogenic- and biogenic emissions. Ruddiman et al. (2011) and Sapart et al. (2012) estimated CH_4 emission change due to anthropogenic land use changes, which shows a good agreement with long-term CH_4 increasing trend. However, there is no high-resolution reconstruction of past population and land use area, and consequently large uncertainties of CH_4 emission from land use change impede identification of any shorter scale changes.

The early Holocene is suitable period to study natural CH_4 controls under Holocene interglacial climate condition. Since there was only negligible human population and relevant CH_4-emitting anthropogenic activities (e.g., Goldewijk et al., 2010; Kaplan et al., 2011) during this time, the early Holocene CH_4 changes must have occurred mostly due to the natural causes. Understanding natural controls could contribute to better constrain the human-induced CH_4 changes. However, high-resolution study for the early Holocene has not been carried out extensively so far, except for the prominent cooling event at 8200 years BP (Spahni et al., 2003; Kobashi et al., 2007; Ahn et al., 2014). Earlier studies mainly focused on long-term change, attributing the major control to low latitude hydrology based on regional climate records that show wetter climate in tropics during the early Holocene (Blunier et al., 1995; Brook et al., 2000; Chappellaz et al., 1993, 1997). Therefore, in this study we present a new high-resolution CH_4 record during the early Holocene to investigate natural control mechanisms under interglacial condition. It should be noted that environmental boundary conditions of the early Holocene were not identical to those of the late Holocene. The global sea level was rising throughout the early Holocene and there were still remnant ice sheets in the north America.

2 Materials and Methods

In this study we used ice samples from a Siple Dome deep ice core (SDMA) drilled from 1997 to 1999 on the Siple Coast, West Antarctica (81.65°S, 148.81°W; 621m elevation) (Taylor et al., 2004). The SDMA samples were collected and cut at National Ice Core Laboratory (NICL, Denver, Colorado, USA) from January to February of 2013. Since brittle zone of SDMA ice starts below 400 m depth (Gow and Meese, 2007) that makes some part of ices fractured and/or cracked internally. Hence the samples were carefully collected from unbroken ices during the sample preparation at NICL. The samples were packed in isothermal foam boxes with numerous eutectic gels, and shipped to South Korea via expedited air freight. Temperature loggers were enclosed within the isothermal boxes to record the temperature change inside during the shipping, and it showed the temperatures were maintained below -25℃. The boxes were picked up directly just after custom clearance at the airport and then the ice samples were stored in a walk-in freezer at Seoul National University (SNU, Seoul, South Korea) that was

maintained below -20℃. We measured 295 individual ice samples from 156 depth intervals from 518.87 to 718.83 m, covering from 8.36 to 20.25 ka after synchronizing to the Greenland Ice Core Chronology 2005 (GICC05, Rasmussen et al., 2006). All samples were duplicated, so that our final CH_4 data were presented by averaging the results of duplicate analysis from the same depth and the analytical uncertainty of each data point is estimated by standard error of the mean of duplicate pairs. The air occluded in ice was extracted by a melting and refreeze process under vacuum. Ice samples were prepared in a walk-in freezer in the morning of each experiment day, and trimmed the outermost >2 mm to eliminate potential contamination by ambient air during the storage. Then the samples were moved to the laboratory and placed in glass sample containers. The sample containers (sample flask hereafter) were custom-made glass flasks welded to stainless steel flange, and attached to the vacuum line with a copper gasket. The sample flasks were partially submerged into a chilled ethanol bath during ice insert and attaching to the line for preventing temperature increase by laboratory air. After that all flasks were evacuated at least 40 minutes, the ice samples were melted by submerging the sample flasks in a warm water bath. Melting process was usually completed within 30 minutes. The sample flasks were then submerged in the cold ethanol bath chilled to around -82℃ for more than an hour to refreeze. During the refreezing, we carried out GC pre-running (20 injections) and daily calibration that normally took 90 minutes. The ethanol temperature rose up to -55℃ just after submerging the flasks, and it was chilled to below -65℃ before expansion of the air in the flasks. The extracted air in the head space was expanded into a gas chromatograph (GC) equipped with a flame ionization detector (FID) to measure CH_4 mixing ratio. The GC linearity was tested by a series of inter-tank calibration using four working standard air cylinders (395.5, 721.3, 895.0, and 1384.9 ppb CH_4 in NOAA04 scale, Dlugokencky et al., 2005). Daily GC calibration curve was determined by measurements of a working standard having the closest CH_4 mixing ratio of expected value from the samples; in this study we used 721.3 ppb CH_4 standard for samples of the early Holocene. To account for system condition change throughout experiments (i.e., influence by water vapor), we calibrated with a standard air six times before and after sample measurements. The detailed configuration of the vacuum line and GC is described in another paper (Yang et al., in preparation).

To estimate our daily blank offset, we used four bubble-free blank ices every day, instead of interpolating between days of blank analysis (Mitchell et al., 2011). The blank ice was made by chilling the degassed ultrapure water (resistivity > 18.2 MΩ·cm at 25°C) slowly from bottom in a closed stainless steel chamber. The daily blank offset is calculated from the mean of the four blank results ranging from 5 to 15 ppb, and it reflects any daily offsets by contaminants, leaks, and any different GC conditions. The exact cause of this blank offset is currently not clear, but the four blank results agree well each other, yielding the intra-day standard error of the mean of 2.0 ± 1.0 ppb. This 'intra-day' blank offset is much smaller than the 'inter-day' offset, which implies that conditions of each sample flask are rather constant within a day, and vary systematically day by day. Since every single data point is obtained by analysis of at least in duplicate, the intra-day blank offset for one depth is reduced by a factor of √2. The robustness of our final results was proven by re-analysis of eight duplicates at adjacent depths (< 10 cm) 8 to 80 days after the first analysis. The difference of the mean of duplicates between the time intervals was 1.9 ppb on average (pooled standard deviation of 1.4 ppb). The good reproducibility of our results demonstrates that our blank correction method is reliable.

Mass dependent (gravitational) fractionation within firn layer (Craig et al., 1988; Schwander, 1989) was corrected by using the nitrogen isotope ratio ($\delta^{15}N$) of atmospheric N_2 occluded in bubbles. Siple Dome $\delta^{15}N$ records show a mean enrichment of 0.23 ± 0.01 ‰ during the early Holocene (Severinghaus et al., 2009) and result in a slight decrease of CH_4 by 1.97 ± 0.15 ppb, which we added to all our measurements to correct the gravitational fractionation.

Different solubility of each gas species cause preferential dissolution of a gas having higher solubility than others, and consequently it makes the mixing ratio of extracted air different from that trapped originally within the ice (solubility effect hear after). As solubility of CH_4 is higher than the other major component of air – nitrogen (N_2), oxygen (O_2), Argon (Ar), the solubility effect lowers the CH_4 mole fraction of the extracted air and needs to be corrected properly. At the early stage of method development, we derive theoretically the solubility effect by using Henry's Law in a closed- and chemically equilibrated condition. After applying this theoretical solubility correction, we observed that SDMA CH_4 data measured at SNU are lower than SDMA CH_4 records from OSU by ~3 ppb in average. Hence we compared the theoretical solubility correction with that obtained empirically from the second gas extraction (following the method described in Mitchell et al., 2011) and found that a correction factor of 1.0058 from the theoretically- to empirically-driven solubility effect. Further details on correction method will be discussed in our manuscript in preparation (Yang et al., in preparation).

Our new Siple Dome CH_4 data has the currently third highest temporal resolution of Antarctic CH_4 records covering the early Holocene after the WAIS Divide continuous (~2 years, Rhodes et al., 2015) and discrete (~20 years, WAIS Divide members, 2015) records. To check reliability of the record we compared our data set with previous SDMA measurement at Oregon State University (OSU) for 8.4 to 9.1 ka period when the two records are overlapped. The OSU CH_4 record was measured with a temporal resolution of 8 years with precision of ±2.8 ppb (Mitchell et al., 2011; Ahn et al., 2014). Resulting mean offset between two data set is ~0.6 ppb, which lies within analytical uncertainty range of both institutes. Therefore, we merge the two records to make the SDMA CH_4 composite data. Fig. 1 presents the SDMA data points during the early Holocene period (119 depths, 518.87 – 623.38 m).

3. Result and Discussion

3.1 Millennial scale variability

To extract millennial-scale variability, we carried out spectral analysis using REDFIT program (Schulze and Mudelsee, 2002) and moderate (over 90% significance level) powers were found at ~1340, 401, 309, and 96-year period. Given the ~42 years of gas age distribution of SDMA (Ahn et al., 2014), it would not reliable to study centennial scale variability. Thus we produced annual data by interpolation and then calculated 250-year running means to smooth high frequency components having shorter period than 309-year. Then the smoothed time series was filtered with a high-pass window (cut off period of 1800 years) to study millennial scale variability throughout the early Holocene. For comparison, the same processing scheme

was applied to WAIS Divide time series and we observed that Siple Dome and WAIS Divide CH_4 anomalies share similar millennial scale variability, confirming reliability of both our data and observed millennial scale changes (Fig. 2).

The CH_4 anomalies demonstrate millennial scale minima at ~8.2, 9.3, 10.2 and 11.0 ka, which occurred in nearly 1000-year spacing. Each minimum is accompanied by depletion of water stable isotope ratio ($\delta^{18}O_{ice}$) from NGRIP ice core, which implies climate cooling in Greenland. A close relationship between CH_4 and Greenland $\delta^{18}O_{ice}$ has been previously reported in glacial-interglacial cycles and Dansgaard-Oeschger (DO) events during the last glacial period (e.g., Brook et al., 1996, 2000; Blunier and Brook, 2001; Chappellaz et al., 1993, 2013; EPICA Community Members, 2006). However, it has not been confirmed at interglacial climate conditions during the Holocene. Mitchell et al. (2011) found no significant correlation with Greenland climate in multi-decadal scale during the late pre-industrial Holocene (LPIH), possibly because LPIH CH_4 budget is also affected substantially by anthropogenic emissions (e.g., Ferretti et al., 2005; Mischler et al., 2009; Mitchell et al., 2013; Sapart et al., 2012). In contrast, we observe a significant positive correlation ($r = 0.57$, $p = 0.06$) between the millennial-scale change of Siple Dome CH_4 and NGRIP $\delta^{18}O_{ice}$ during the early Holocene. The correlation coefficient between the smoothed- and filtered time series of SDMA CH_4 (before synchronization to GICC05) and NGRIP $\delta^{18}O_{ice}$ was calculated for the 7.8-11.5 ka by interpolating to the original ages of SDMA CH_4 composite, with a reduced degree of freedom.

The previous SDMA gas chronology (Brook et al., 2005; Severinghaus et al., 2009) was synchronized to GICC05 age scale by setting age tie-points with stable water isotope ($\delta^{18}O$) record from the North Greenland Ice Core Project (NGRIP) ice cores during the abrupt climate change events of the Preboreal Oscillation (PBO) and the 8.2 ka event, given that both events have been proved to be synchronous with CH_4 change (Kobashi et al., 2007, 2008). The synchronization between the tie points was done by linear interpolation of age differences between the synchronized- and the previous ones, which range from -114 to 28 years. After synchronizing to GICC05 scale, the correlation coefficient between SDMA CH_4 composite and NGRIP $\delta^{18}O_{ice}$ increases to $r = 0.74$ ($p < 0.01$) (Fig. S1).

According to atmospheric modelling studies, abrupt cooling in the North Atlantic regions can alter atmospheric circulation and to cause southward migration of the mean latitudinal position of the Intertropical Convergence Zone (ITCZ) (e.g., Chiang and Bitz, 2005; Broccoli et al., 2006; Cvijanovic and Chiang, 2012). The climatic teleconnection between northern North Atlantic and low latitude regions is shown by climate proxies. Sediment reflectance record from Cariaco Basin shows increased rainfall and humidity – which is due to southward displacement of ITCZ – corresponding to the 8.2, 9.3, and 10.9 ka abrupt cooling event,,as revealed in previous studies for the different time periods (Peterson et al., 2000; Haug et al., 2001; Fleitmann et al., 2007; Deplazes et al., 2013). The southward displacement of ITCZ leads further weakening of Asian and Indian summer monsoons and probably reduces CH_4 emission from northern tropical wetlands. The ^{18}O enrichments of speleothem in Dongge Cave (China), Qunf Cave (Oman), and Hoti Cave (Oman, not shown, Neff et al., 2001) occurred at similar timing with abrupt cooling in Greenland at 8.2, 9.3, and 10.9 ka, which indicate the reduction of monsoonal rainfall at northern tropical wetlands. The speleothem records from Chinese and Oman caves seem to lag by ~100-200 years after the CH_4 change at ~9.3 ka, but this lies within chronological uncertainties of ~200-400 years at around ~9.0 ka (Dykoski et al., 2005; Fleitmann et al., 2007).

Moreover, sediment Ba/Ca ratio from Gulf of Guinea demonstrates concurrent decrease of west African monsoon (Weldeab et al., 2007). The record indicates that precipitation over the major wetland area was reduced and in turn it would lower the wetland CH_4 emissions in NH. In the meanwhile, an inverse relationship is observed from the Eastern Brazilian speleothem data (Lapa Grande Cave, Strikis et al., 2011) that demonstrate the increase of precipitation at the time of abrupt CH_4 decrease occurred as a result of southward migration of ITCZ. Rhodes et al. (2015) pointed out that strong southward migration of ITCZ could induce an abrupt CH_4 increase from southern hemisphere during the HS 1, 2, 4, and 5 events. Sperlich et al. (2015) also found that a sharp CH_4 peak at Greenland Interstadial 21.2 (~85 ka) was occurred by emission from Asian and South American wetlands. However, considering the orbital parameters that indicate maximum summer insolation in NH while minimum in SH during the early Holocene, it can be inferred that contribution of SH wetland emission was relatively weak and overcompensated by reduction of NH emission.

The possibility that the observed CH_4 minima were caused by reduction of northern extra-tropical sources is not supported by previous modelling study. Zürcher et al. (2013) found that abrupt cooling in Greenland and northern high latitudes by large freshwater input causes boreal peatland CH_4 emission to decrease substantially, which explains ~23% of abrupt CH_4 decrease (~80 ppb) during the 8.2 ka event. If we assume linear scaling of the model response, it implies that boreal peatland source change only accounts for ~23% of total CH_4 change during the rest of CH_4 decrease events. Given the meltwater pulses during the early Holocene before the 8.2 ka event are more than 10 times weaker (Teller and Leverington, 2004) than that corresponding to the 8.2 ka event, we consider the boreal emission change is not the major cause of CH_4 local minima.

Previously, Björck et al. (2001) found the climate cooling in the northern Atlantic and Santa Barbara Basin occurred with solar-forcing change at ~10.3 ka. However, the proxy data in Figure 2 show no clear indication of southward migration of ITCZ position and changes in Asian, Indian, African, and South American summer monsoon intensity associated to ~10.2 ka cooling (Fig. 2b-f). Moreover, there was no distinct change in $\Delta\varepsilon_{LAND}$ at that time, a proxy of global terrestrial respiratory fractionation of atmospheric O_2, which is affected by low latitude surface hydrology (Severinghaus et al., 2009). This paleoproxy record suggests that changes in precipitation and surface hydrology in the northern tropics may have not changed significantly during around the 10.2 ka. Instead, there are two small decreases at ~9.9 and ~10.6 ka as shown in Dongge cave deposit record (Fig. 2d). These episodes are not likely associated with the CH_4 minimum at 10.2 ka because the timing differences between the CH_4 minimum and reductions of Asian summer monsoon intensity are beyond the chronological uncertainty. The age uncertainty of Dongge Cave deposits is ±77 years (2 sigma error; Dykoski et al., 2005), and the estimated error of SDMA CH_4 gas age in this study is less than ~150 years (see Supplement and Fig. S3). The climate teleconnection between North Atlantic and tropical hydrology at 10.2 ka might not have been sufficiently strong enough to change the low latitude climate. Weak cooling around the North Atlantic region can be a candidate, given that NGRIP $\delta^{18}O_{ice}$ records demonstrate smaller amplitude negative anomaly during ~10.2 ka event than those of 8.2 and 9.3 ka. The amplitude of $\delta^{18}O_{ice}$ changes at 10.2 ka of the high-pass filtered GRIP and GISP2 records does show smaller variability than those at 8.2 and 9.3 ka cooling events, but larger than the variability at 10.9 ka (Fig. S2). Hence, the "weak cooling" speculation is not fully supported by the other Greenland ice core records. Although there appears to have been no strong change in low latitude

hydrology at 10.2 ka, the amplitude of CH_4 decrease at 10.2 ka is similar order to the other millennial events. Given that no clear reduction of the Asian, Indian, and African monsoon intensity is observed, it may imply the CH_4 decrease at 10.2 ka was controlled by other processes than the monsoon circulation change. If the climate proxy from Dongge cave reflects rather regional climate changes, monsoonal rainfalls and surface hydrology of other regions could be responsible for CH_4 decrease.

There should be an ultimate cause of the CH_4 and climate change in the early Holocene. Previous works have suggested an important role of solar forcing during the Holocene (e.g., Björck et al., 2001; Bond et al., 1997, 2001). Bond et al. (1997) reported four large ice-rafted debris (IRD) drifts occurred at ~8.1, 9.4, 10.3 and 11.1 ka caused by surface cooling of North Atlantic Ocean. They found that the ocean surface cooling and the IRD events are closely related to cooling over the Greenland. Figure 2 shows that each IRD event (maxima in hematite stained grain) occurred concurrently with minima of NGRIP $\delta^{18}O_{ice}$ record within age uncertainty. Then the Greenland cooling leads southward shift of ITCZ and in turn it changes wetland CH_4 emission in low latitudes. Bond et al. (2001) found that IRD maxima during the Holocene coincide with solar activity minima. The authors suggested that solar forcing could affect the climate change around the North Atlantic Ocean (and Greenland), through amplification by changes in sea ice and/or deep water formation. A close interplay between solar activity and monsoon intensity has been observed in previous studies using the Chinese and Oman speleothem records during the Holocene (Neff et al., 2001; Wang et al., 2005; Gupta et al., 2005), even on multi-decadal time scales (Agnihotri et al., 2002). However, the forcing mechanism of solar activity on the North Atlantic and global climate is not well understood. Jiang et al. (2015) found positive correlations between North Atlantic SST and solar forcing inferred from plaeoproxies (^{14}C and ^{10}Be) for the last 4000 years, while the correlation disappears during the mid- and early Holocene. They hypothesized that climate sensitivity to solar forcing is high for cooler climate. As evidenced above, the early Holocene CH_4 minima were likely triggered by anomalous low solar activity, but future study is needed to make it more conclusive.

Meanwhile, shifting to El Nino-like SST condition was suggested as another mechanism that changes tropical rainfall pattern (Marchitto et al., 2010). According to modern atmospheric observation, El Niño condition leads drying conditions in low latitude wetlands in Africa, Asia, and America (e.g., Dai and Wigley, 2000; Lyon and Barnston, 2005; Hodson et al., 2011), which reduces tropical CH_4 emissions. Thus, we could speculate that both the ITCZ migration and El Niño-like SST change affected the tropical surface hydrology and CH_4 emission. According to Holocene ENSO activity reconstructions by Moy et al. (2002), no ENSO event was recorded during the early Holocene until around 7 ka, except weak ENSO events during 10.4-10.1 ka, where abrupt CH_4 decrease is observed without significant changes in ITCZ and NH monsoon intensities. Mitchell et al. (2011) observed a significant positive correlation between CH_4 and Pacific Decadal Oscillation (PDO) variability during the late Holocene. It has been reported that PDO modulates the wet/dry impact of ENSO depending on phase relationship between ENSO and PDO (e.g., Wang et al., 2014 and references therein). The Holocene PDO reconstruction from sediment grain size analysis by Kirby et al. (2010) shows PDO-related drying intervals in North America during 9.5-9.1, 8.9-8.6, and 8.3-7.8 ka, which overlap the CH_4 minima at 8.2 and 9.3 ka present in this study.

3.2. Inter-polar difference of CH_4 during the early Holocene

We calculated inter-polar difference (IPD) of CH_4 to trace the latitudinal source distribution change during the early Holocene. The currently available high-resolution CH_4 records covering the early Holocene are SDMA discrete (this study), WAIS Divide discrete (WAIS Divide project members, 2015), WAIS Divide continuous (Rhodes et al., 2015), NEEM discrete (Chappellaz et al., 2013) and NEEM continuous data (Chappellaz et al., 2013). Among the Antarctic records, we consider WAIS continuous records are more reliable than WAIS discrete ones because WAIS discrete data covering the early Holocene were measured in a different institute (Penn State University, PSU), showing a pooled standard deviation of ~7.3 ppb (1σ). In addition, there is an unexplained offset between WAIS CH_4 measured in OSU and PSU lab by ~9.9 ppb (Rhodes et al., 2015), which is larger than that observed between SNU and OSU SDMA data sets. Regarding the Greenland side, we use NEEM discrete records because there are discrepancies between continuous- and discrete data in some intervals, but also because the NEEM continuous record is not exactly "continuous". Hence, here we regard the NEEM discrete, Siple Dome discrete, and WAIS Divide continuous data as more reliable ones than the others to reconstruct IPD during the early Holocene.

Precise synchronization is crucial for direct comparison between data sets which have high frequency variations. For synchronizing between Antarctic (Siple Dome and WAIS Divide continuous) and NEEM records, the NEEM CH_4 record (~11-year resolution on average) is chosen as reference. Synchronization was done by two steps: First, we made initial synchronization between the Antarctic and NEEM data by setting match points at the midpoint of abrupt CH_4 change, and then we linearly interpolated the age offset of each match point for the rest of data points. Then we applied a Monte Carlo simulation to find a maximum correlation. Both data sets were resampled every 30 years, and each point was randomly disturbed (assuming a normal distribution with 1 sigma of 30 years). By doing so 1000 different time series were created, and one set having a maximum correlation with NEEM data was chosen. Criteria for "best fit" is correlation coefficient of 0.8 with NEEM original age scale, so that a maximum correlation less than 0.8 was discarded. This procedure was repeated to make 20 sets of maximum correlation time series, and the mean ages of 20 replicate simulations were set to synchronized age scale. Temporal uncertainty (synchronizing error) was determined for each point as 1 standard deviation of 20 replicates and CH_4 uncertainty includes analytical error of the both records (4.3 ppb for NEEM discrete /1.4 ppb for SDMA / 1.5 ppb for WAIS continuous, 1 sigma). Since IPD calculation is very sensitive to high frequency variability of CH_4 records from both poles, and it is difficult to reconstruct reliable IPD in short time scales, all IPD records in this study were filtered by a 1000-year low-pass window to discuss multi-centennial to millennial scale change. As discrete measurements are regarded as more accurate than continuous ones in absolute sense, WAIS continuous data were calibrated against to Siple Dome data instead of WAIS discrete record, because Siple Dome records were more rigorously tested for its reproducibility, and also compared with OSU measurements that shows small offset during the early Holocene interval.

The IPDs from those three data sets are plotted in grey (NEEM discrete – Siple Dome, IPD-1 hereafter) and green (NEEM discrete – WAIS continuous, IPD-2 hereafter) in Figure 3. Resulting IPD-1 and IPD-2 show long-term increase from 11.5 to 9.9 ka, which indicates that boreal source contribution enhanced. However, IPD-1 shows a sharp increase during PBO followed

by decrease until ~10.7 ka, and in the latter case both IPDs differ beyond 95% envelope (from 10.4 to 10.8 ka). This is because Siple Dome discrete data are higher than WAIS continuous data during this interval. Similarly, the small peak of IPD-1 at ~11.1 ka that is not seen in IPD-2 may be caused by offset between Siple- and WAIS data during 11.0 to 11.3 ka. By using our new IPDs and the reliable highly resolved CH_4 records (NEEM discrete – SDMA discrete / WAIS continuous), we ran a simple 3-box CH_4 source distribution model to quantify how much the boreal and tropical source strengths were changed. Here we used the same box model employed in Chappellaz et al. (1997) and Brook et al. (2000). Briefly, the model contains 3 boxes; northern extra-tropical latitude (30-90°N, N-box), tropical (30°S-30°N, T-box), and southern extra-tropical latitude boxes (30-90°S, S-box). CH_4 mixing ratios in 3 boxes (in Tg box^{-1}) were determined from CH_4 mixing ratio of Antarctica and Greenland. The mean CH_4 mole fraction of N-box (30-90N) is not identical to that of Greenland ice core record, given the latitudinal CH_4 distribution (e.g., Fung et al., 1991). To derive the N-box CH_4, we followed the assumption of Chappellaz et al. (1997), where the authors assumed that difference between Greenland and the mean N-box CH_4 is 7% of IPD. Hence here the N-box CH_4 is calculated by subtracting 7% of IPD from the Greenland mixing ratio. T-box mixing ratio is inferred by assuming that the S-box emission is constant of 15 Tg yr^{-1} (Fung et al., 1991). Emission from each box (Tg yr^{-1}) is then estimated by using the mixing ratios of the boxes, lifetime of CH_4 in each box, and transport times among the boxes. The modelled emission changes in NH extratropical- and tropical boxes from IPD-1 are plotted in Figure 4 (see Fig. S3 for results from IPD-2). The model reveals decreasing tropical sources (accounting for the largest portion in CH_4 budget), while enhancing NH extratropical emissions. The tropical emission was elevated by ~8 Tg yr^{-1} from the onset of the Holocene to its maximum at 10.6 ka, followed by ~15 g yr^{-1} reduction to ~111 Tg yr^{-1} at 9.5 ka. Tropical emission decrease is also observed in IPD-2 from 134 to 115 Tg yr^{-1} during the 11.5-10.0 ka, but this change is not significant in 95% confidence range (Fig. S3 and Table S2). The long-term decreasing trend follows the NH summer insolation change. This covariation may reflect the insolation-driven changes in multi-millennial timescale (e.g., Loulergue et al., 2008; Guo et al., 2012). CH_4 flux from NH extratropical box increased from ~57 Tg yr^{-1} (11.5 ka) to ~70 Tg yr^{-1} (9.5 ka), showing a local minimum of ~63 Tg yr^{-1} at 10.7 ka. Also plotted in Figure 4 is boreal source fraction, defined as ratio of N-box emission to total source emissions. It shows a significant increase from ~30% at 11.5 ka to ~35% at 9.5 ka. The box model results from IPD-2 demonstrate increase of NH extratropical emission from 60 to 71 Tg yr^{-1}, and hence increase of the boreal source fraction from 29 to 35% during the 11.5 to 10.0 ka interval.

This conclusion is supported by proxy-based temperature reconstructions that indicate a gradual warming in northern extratropical region (30N-90N) until ~9.6 ka, while tropical temperature remains stable (Marcott et al., 2013). The climate warming in northern high latitudes caused ice sheet retreat (e.g., Dyke, 2004) and enhanced CH_4 emission from boreal permafrost by forming new wetlands in mid- to high latitudes (e.g., Gorham et al., 2007; Yu et al., 2013) and accelerating microbial decomposition of organic materials (e.g., Christensen et al., 2004; Schuur et al., 2015). Thermokarst lakes created by thawing ice wedges and ground ices in Alaskan- and Siberian permafrost has been suggested as a source of CH_4 (e.g., Walter et al., 2006, 2007; Brosius et al., 2012). The modelled enhancement of NH extratropical emission of ~13 Tg yr^{-1} is greater than the CH_4 release of 8.2 Tg yr^{-1} from thermokarst lake thawing, which is estimated based on present-day observations (Walter et al., 2014). Since most thermokarst lakes are located in NH high latitude regions (e.g., Walter et al., 2006; 2014), it

may indicate that other sources, such as northern peatlands or mid-latitude wetlands, should contribute to increasing NH extratropical emission. Our results are consistent with previous findings of CH_4 stable isotope analysis. Fischer et al. (2008) found that increase of boreal source contribution is required to explain the more depleted $\delta^{13}C$-CH_4 during Preboreal Holocene than the Younger Dryas interval. Sowers (2010) extended the CH_4 isotopic ratio into the entire Holocene that displayed a gradual decrease of $\delta^{13}C$-CH_4 by ~2 ‰ from 10.5 to 4 kyr BP, which was attributed to progressive expansion of NH high latitude sources.

3.3. Comparison with late Holocene variability

We compared amplitude of CH_4 variability between the early- and the late Holocene in multi centennial to millennial time scales. Figure 5 shows amplitude spectrum and root mean square (RMS) amplitude for the early Holocene and the late Holocene, respectively. The amplitude of the early Holocene CH_4 change is ~10 ppb and does not change greater except for PBO and the 8.2 ka event, while the late Holocene spectrum shows smaller amplitude than early Holocene for shorter-term change and larger for longer-term fluctuation. Late Pre-Industrial Holocene (LPIH) CH_4 amplitude is elevated to early Holocene level from ~0 C.E. (~2.0 ka), and increases up to higher from ~1450 C.E. (~0.5 ka).

The reason of low amplitude variability during 3.5 to 1.2 ka, or why the early Holocene CH_4 variability is larger than this period, is probably related to different orbital configuration in both time periods. Previous studies found covariation between CH_4 amplitude and NH summer insolation change, reflecting that mean temperature of the warmest seasons is an important factor of CH_4 emission, during the interstadial conditions (Flückiger et al., 2004; Baumgartner et al., 2014). Combined with elevated summer insolation in Northern Hemisphere (NH) and with climate warming in NH extratropics, the amplified variability of the early Holocene may suggest that CH_4 control by NH wetlands was likely stronger than the late Holocene period. Meanwhile, lower summer insolation during the late Holocene might induce diminished CH_4 amplitude. This evidence indicates the natural forcing in centennial- to millennial time scales is reduced in the late Holocene, given that the atmospheric CH_4 budget during 3.5-1.2 ka (604.9 ppb) is similar to that during 9.0-7.6 ka (628.6 ppb), and that anthropogenic emission is greater in later Holocene than the early Holocene. Abrupt increase of CH_4 amplitude since ~800 C.E. (1.2 ka) is likely driven by increasing anthropogenic contribution, which is consistent with anthropogenic emission scenario based on past population and agricultural activity (Mitchell et al., 2013). Also superimposed are short-term cooling events during Little Ice Age, making CH_4 variability greater.

4. Conclusion and summary

We reconstructed a new high resolution CH_4 record during the early Holocene from Siple Dome ice core, Antarctica, to study millennial-scale CH_4 variability and its natural controls under Holocene interglacial condition. Since the new SDMA data agree well with previous measurements at OSU, we made SDMA CH_4 composite data covering ~7.7 to 11.6 ka. We found

four millennial scale CH_4 minima accompanied with Greenland cooling, changes in ITCZ position and reduced Asian and Indian monsoon intensities. The observed evidences suggest that low latitude hydro climate changes were closely related to millennial scale CH_4 minima. Further, this study presented the millennial scale change of IPD, which was calculated from high resolution discrete dataset of NEEM and SDMA. Here we reported for the first time the IPD increase from the onset of the Holocene to ~9.9 ka following the temperature rise in NH extra-tropical regions. The three-box model demonstrates that elevated emission from NH extratropics and reduction of tropical sources, resulting the increased contribution of the NH extra-tropical sources. Finally, we observed that RMS amplitude of earlier part of the late Holocene is smaller than that of the early Holocene, which may be attributed to different orbital parameters.

Acknowledgements. Financial support was provided by the Basic Science Research Program through the National Research Foundation of Korea (NRF) (NRF-2015R1A2A2A01003888) and Korea Polar Research Institution (KOPRI) research grant (PD12010 and PE15010). This work was also supported by the US National Science Foundation Grant PLR 1043518. We appreciate all the efforts of sample cutting and shipping of the Siple Dome ice core by Brian Bencivengo, Richard Nunn, and Geoffrey Hargreaves of National Ice Core Laboratory, Denver, Colorado. We sincerely thank to Yoo-Hyeon Jin, Jinhwa Shin, and Hun-Gyu Lee for their laboratory assistance and helpful discussions. Thanks should go to Heejo Lee for her help in preparing English manuscript. We are grateful to Mark Twickler and the NICL Science Management Office for providing the Siple Dome ice core samples, the collection of which was supported by the US National Science Foundation.

Data availability

The early Holocene Siple Dome CH_4 data will be available on NOAA Paleoclimatology database and PANGAEA data repository.

References

Agnihotri, R., Dutta, K., Bhushan, R., and Somayajulu, B. L. K.: Evidence for solar forcing on the Indian monsoon during the last millennium, Earth Planet. Sci. Lett., 198, 521-527, 2002.

Ahn, J., Brook, E. J., and Buizert, C.: Response of atmospheric CO_2 to the abrupt cooling event 8200 years ago, Geophys. Res. Lett., 41, 604-609, 2014.

Andreae, M. O., and Merlet, P.: Emission of trace gases and aerosols from biomass burning, Global Biogeochem. Cycles, 15, 955-966, 2001.

Baumgartner, M., Kindler, P., Eicher, O., Floch, G., Schilt, A., Schwander, J., Spahni, R., Capron, E., Chappellaz, J., Leuenberger, M., Fischer, H., and Stocker, T. F.: NGRIP CH_4 concentration from 120 to 10 kyr before present and its relation to a $\delta^{15}N$ temperature reconstruction from the same ice core, Clim. Past, 10, 903-920, 2014.

Berger, A., and Loutre, M. F.: Insolation values for the climate of the last 10 million years, Quat. Sci. Rev., 10, 297-317, 1991.

Berkelhammer, M., Sinha, A., Stott, L., Cheng, H., Pausata, F., and Yoshimura, K.: An abrupt shift in the Indian Monsoon 4000 years ago, Geophys. Monogr. Ser., 198, 75-87, 2012.

Björck, S., Muscheler, R., Kromer, B., Andresen, C. S., Heinemeier, J., Johnsen, S. J., Conley, D., Koç, N., Spurk, M., and Veski, S.: High-resolution analyses of an early Holocene climate event may imply decreased solar forcing as an important climate trigger, Geology, 29, 1107-1110, 2001.

Blunier, T., Chappellaz, J., Schwander, J., Stauffer, B., and Raynaud, D.: Variations in atmospheric methane concentration during the Holocene epoch, Nature, 374, 46-49, 1995.

Blunier, T., and Brook, E. J.: Timing of millennial-scale climate change in Antarctica and Greenland during the last glacial period, Science, 291, 109-112, 2001.

Broccoli, A. J., Dahl, K. A., and Stouffer, R. J.: Response of the ITCZ to northern hemisphere cooling, Geophys. Res. Lett., 33, L01702, 2006.

Bond, G., Kromer, B., Beer, J., Muscheler, R., Evans, M. N., Showers, W., Hoffmann, S., Lotti-Bond, R., Hajdas, I., and Bonani, G.: Persistent solar influence on north Atlantic climate during the Holocene, Science, 294, 2130-2136, 2001.

Brook, E. J., Sowers, T., and Orchardo, J.: Rapid variations in atmospheric methane concentration during the past 110,000 years, Science, 273, 1087-1091, 1996.

Brook, E. J., Harder, S., Severinghaus, J. P., Steig, E. J., and Sucher, C. M.: On the origin and timing of rapid changes in atmospheric methane during the last glacial period, Global Biogeochem. Cy., 14, 559-572, 2000.

Brook, E. J., White, J. W. C., Schilla, A. S. M., Bender, M. L., Barnett, B., Severinghaus, J. P., Taylor, K. C., Alley, R. B., and Steig, E. J.: Timing of millennial-scale climate change at Siple Dome, West Antarctica, during the last glacial period, Quat. Sci. Rev., 24, 1333-1343, 2005.

Brosius, L. S., Walter Anthony, K. M., Grosse, G., Chanton, J. P., Farquharson, L. M., Overduin, P. P., and Meyer, H.: Using the deuterium isotope composition of permafrost meltwater to constrain thermokarst lake contributions to atmospheric CH_4 during the last deglaciation, J. Geophys. Res., 117, G01022, 2012.

Chappellaz, J., Chappellaz, J., Blunier, T., Raynaud, D., Barnola, J. M., Schwander, J., and Stauffer, B.: Synchronous changes in atmospheric CH_4 and Greenland climate between 40 and 8 kyr BP, Nature, 366, 443-445, 1993.

Chappellaz, J., Blunier, T., Kints, S., Dällenbach, A., Barnola, J. M., Schwander, J., Raynaud, D., and Stauffer, B.: Changes in the atmospheric CH_4 gradient between Greenland and Antarctica during the Holocene, J. Geophys. Res., 102, 15987-15997, 1997.

Chappellaz, J., Stowasser, C., Blunier, T., Baslev-Clausen, D., Brook, E. J., Dallmayr, R., Faïn, X., Lee, J. E., Mitchell, L. E., Pascual, O., Romanini, D., Rosen, J., and Schüpbach, S.: High-resolution glacial and deglacial record of atmospheric methane by continuous-flow and laser spectrometer analysis along the NEEM ice core, Clim. Past, 9, 2579-2593, 2013.

Chiang, J. C. H., and Bitz, C. M.: Influence of high latitude ice core on the marine intertropical convergence zone, Clim. Dynam., 25, 477-496, 2005.

Chiang, J. C. H., Cheng, W., and Bitz, C. M.: Fast teleconnections to the tropical Atlantic sector from Atlantic thermohaline adjustment, Geophys. Res. Lett., 35, L07704, 2008.

Christensen, T. R., Johansson, T., Jonas Åkerman, H., Mastepanov, M., Malmer, N., Friborg, T., Crill, P., and Svensson, B. H.: Thawing sub-arctic permafrost: effects on vegetation and methane emissions, Geophys. Res. Lett., 31, L04501.

Cvijanovic, I., and Chiang, J. C. H.: Global energy budget changes to high latitude North Atlantic cooling and the tropical ITCZ response, Clim. Dynam., 40, 1435-1452, 2013.

Craig, H., Horibe, Y., and Sowers, T.: Gravitational separation of gases and isotopes in polar ice caps, Science, 242, 1675-1678, 1988.

Cruz, F. W., Burns, S. J., Karmann, I., Sharp, W. D., Vuille, M., Cardoso, A. O., Ferrari, J. A., Silva Dias, P. L., and Viana, O.: Insolation-driven changes in atmospheric circulation over the past 116,000 years in subtropical Brazil, Nature, 63-66, 2005.

Dai, A., and Wigley, T. M. L.: Global patterns of ENSO-induced precipitation, Geophys. Res. Lett., 27, 1283-1286, 2000.

Deplazes, G., Luckge, A., Peterson, L. C., Timmermann, A., Hamann, Y., Hughen, K. A., Rohl, U., Laj, C., Cane, M. A., Sigman, D. M., and Haug, G. H.: Links between tropical rainfall and North Atlantic climate during the last glacial period, Nat. Geosci., 6, 213-217, 2013.

Dlugokencky, E. J., Steele, L. P., Lang, P. M., and Masarie, K. A.: The growth rate and distribution of atmospheric methane, J. Geophys. Res., 99, 17021-17043, 1994.

Dlugokencky, E. J., Myers, R. C., Lang, P. M., Masarie, K. A., Crotwell, A. M., Thoning, K. W., Hall, B. D., Elkins, J. W., and Steele, L. P.: Conversion of NOAA atmospheric dry air CH_4 mole fractions to a gravimetrically prepared standard scale. J. Geophys. Res., 110, 2005.

Dlugokencky, E. J., Bruhwiler, L., White, J. W. C., Emmons, L. K., Novelli, P. C., Montzka, S. A., Masarie, K. A., Lang, P. M., Crotwell, A. M., Miller, J. B., and Gatti, L. V.: Observational constraints on recent increases in the atmospheric CH_4 burden, Geophys. Res. Lett., 36, L18803, 2009.

Dlugokencky, E.J., Nisbet, E. J., Fisher, R., and Lowry, D.: Global atmospheric methane: Budget, changes, and dangers, Philosophical Transactions of the Royal Society A, 369, 2058-2072, 2011.

Dyke, A. S.: An outline of North American deglaciation with emphasis on central and northern Canada, in: Quaternary Glaciations - Extent and Chronology Part II: North America, Volume 2, edited by: Ehlers J. and Gibbard, P. L., Elsevier, Amsterdam, 373-424, 2004.

Dykoski, C. A., Edwards, R. L., Cheng, H., Yuan, D., Cai, Y., Zhang, M., Lin, Y., Qing, J., An, Z., and Revenaugh, J.: A high-resolution, absolute-dated Holocene and deglacial Asian monsoon record from Dongge Cave, China, Earth Planet. Sci. Rev., 233, 71-86, 2005.

EPICA Community Members: One-to-one coupling of glacial climate variability in Greenland and Antarctica, Nature, 444, 195-198, 2006.

Etiope, G., Lassey, K. R., Klusman, R. W., and Boschi, E.: Reappraisal of the fossil methane budget and related emission from geologic sources, Geophys. Res. Lett., 35, L09307, 2008.

Ferretti, D., Miller, J. B., White, J. W. C., Etheridge, D. M., Lassey, K. R., Lowe, D. C., MacFarling-Meure, C. M., Dreier, M. F., Trudinger, C. M., van Ommen, T. D., and Langenfelds, R. L.: Unexpected changes to the global methane budget over the past 2000 years, Science, 309, 1714-1717, 2005.

Finkel, R. C., and Nishizumi, K.: Beryllium 10 concentrations in the Greenland Ice Sheet Project 2 ice core from 3-40 ka, J. Geophys. Res., 102, 26699-26706, 1997.

Fischer, H., Behrens, M., Bock, M., Richter, U., Schmitt, J., Loulergue, L., Chappellaz, J., Spahni, R., Blunier, T., Leuenberger, M., and Stocker, T. F.: Changing boreal methane sources and constant biomass burning during the last termination, Nature, 452, 864-867, 2008.

Fleitmann, D., Burns, S. J., Mangini, A., Mudelsee, M., Kramers, J., Villa, I., Neff, U., Al-Subbary, A. A., Buettner, A., Hippler, D., and Matter, A.: Holocene ITCZ and Indian monsoon dynamics recorded in stalagmites from Oman and Yemen (Socotra), Quaternary Sci. Rev., 26, 170-188, 2007.

Flückiger, J., Blunier, T., Stauffer, B., Chappellaz, J., Spahni, R., Kawamura, K., Schwander, J., Stocker, T. F., and Dahl-Jensen, D.: N_2O and CH_4 variations during the last glacial epoch: Insight into global processes, Global Biogeochem. Cycles, 18, GB1020, 2004.

Fung, I., John, J., Lerner, J., Matthews, E., Prather, M., Steele, L. P., and Fraser, P. J.: Three-dimentional model synthesis of the global methane cycle, J. Geophys. Res., 96, 13033-13065, 1991.

Goldewijk, K. K., Beusen, A., and Janssen, P.: Long-term dynamic modelling of global population and built-up area in a spatially explicit way: HYDE 3.1, The Holocene, 1-9. 2010.

Gorham, E., Lehman, C., Dyke, A., Janssens, J., and Dyke, L.: Temporal and spatial aspects of peatland initiation following deglaciation in North America, Quaternary Sci. Rev., 26, 300-311, 2007.

Gow, A. J., and Meese, D.: Physical properties, crystalline textures and *c*-axis fabrics of the Siple Dome (Antarctica) ice core, J. Glaciol., 53, 573-584, 2007.

Grachev, A. M., Brook, E. J., and Severinghaus, J. P.: Abrupt changes in atmospheric methane at the MIS 5b-5a transition, Geophys. Res. Lett., 34, L20703, 2007.

Grachev, A. M., Brook, E. J., Severinghaus, J. P., and Pisias, N. G.: Relative timing and variability of atmospheric methane and GISP2 oxygen isotopes between 68 and 86 ka, Global Biogeochem. Cy., 23, GB2009, 2009.

Guillevic, M., Bazin, L., Landais, A., Stowasser, C., Masson-Delmotte, V., Blunier, T., Eynaud, F., Falourd, S., Michel, E., Minster, B., Popp, T., Prié, F., and Vinther, B. M.: Evidence for a three-phase sequence during Heinrich Stadial 4 using a multi-proxy approach based on Greenland ice core records, Clim. Past, 10, 2115-2133, 2014.

Guo, Z., Zhou, X., and Wu, H.: Glacial-interglacial water cycle, global monsoon and atmospheric methane changes, Clim. Dynam., 39, 1073-1092, 2012.

Gupta, A. K., Das, M., and Anderson, D. M.: Solar forcing on the Indian summer monsoon during the Holocene, Geophys. Res. Lett., 32, L17703, 2005.

Hao, W. M., and Ward, D. E.: Methane production from global biomass burning, J. Geophys. Res., 98, 20657-20661, 1993.

Haug, G. H., Hughen, K. A., Sigman, D. M., Peterson, L. C., and Röhl, U.: Southward migration of the intertropical convergence zone through the Holocene, Science, 293, 1304-1308, 2001.

Hodson, E. L., Poulter, B., Zimmermann, N. E., Prigent, C., and Kaplan, J. O.: The El Niño-Southern Oscillation and wetland methane interannual variability, Geophys. Res. Lett., 38, L08810, 2011.

Hopcroft, P. O., Valdes, P. J., and Beerling, D. J.: Simulating idealized Dansgaard-Oeschger events and their potential impacts on the global methane cycle, Quat. Sci. Rev., 30, 3258-3268, 2011.

Hughen, K. A., Overpeck, J. T., Peterson, L. C., and Trumbore, S.: Rapid climate changes in the tropical Atlantic region during the last deglaciation, Nature, 380, 51-54, 1996.

Jiang, H., Muscheler, R., Björck, S., Seidenkrantz, M. S., Olsen, J., Sha, L., Sjolte, J., Eriksson, J., Ran, L., Knudsen, K. L., and Knudsen, M. F.: Solar forcing of Holocene summer sea-surface temperatures in the northern North Atlantic, Geology, 43, 2015.

Joabsson, A., and Christensen, T. R.: Methane emissions from wetlands and their relationship with vascular plants: an Arctic example, Global Change Biol., 7, 919-932, 2001.

Kaplan, J. O., Krumhardt, K. M., Ellis, E. C., Ruddiman, W. F., Lemmen, C., and Goldewijk, K. K.: Holocene carbon emissions as a result of anthropogenic land cover change, The Holocene, 21, 775-791, 2011.

Kirby, M. E., Lund, S. P., Patterson, W. P., Anderson, M. A., Bird, B. W., Ivanovici, L., Monarrez, P., and Nielsen, S.: A Holocene record of Pacific Decadal Oscillation (PDO)-related hydrologic variability in Southern California (Lake Elsinore, CA), J. Paleolimnol., 44, 819-839, 2010.

Kobashi, T., Severinghaus, J. P., Brook, E. J., Barnola, J. -M., and Grachev, A. M.: Precise timing and characterization of abrupt climate change 8200 years ago from air trapped in polar ice, Quaternary Sci. Rev., 26, 1212-1222, 2007.

Kobashi, T., Severinghaus, J. P., and Barnola, J. -M.: 4±1.5 ℃ abrupt warming 11270 yr ago identified from trapped air in Greenland ice, Earth Planet. Sci. Lett., 268, 397-407, 2008.

Landais, A., Dreyfus, G., Capron, E., Masson-Delmotte, V., Sanchez-Goñi, M. F., Desprat, S., Hoffmann, G., Jouzel, J., Leuenberger, M., and Johnsen, S.: What drives the millennial and orbital variations of $\delta^{18}O_{atm}$?, Quat. Sci. Rev., 29, 235-246, 2010.

Levine, J. G., Wolff, E. W., Jones, A. E., Sime, L. C., Valdes, P. J., Archibald, A. T., Carver, G. D., Warwick, N. J., and Pyle, J. A.: Reconciling the changes in atmospheric methane sources and sinks between the Last Glacial Maximum and the pre-industrial era, Geophys. Res. Lett., 38, L23804, 2011.

Levy II, H.: Normal atmosphere: large radical and formaldehyde concentrations predicted, Science, 173, 141-143, 1971.

Loulergue, L., Schilt, A., Sphani, R., Masson-Delmotte, V., Blunier, T., Lemieux, B., Barnola, J. -M., Raynaud, D., Stocker, T. F., and Chappellaz, J.: Orbital and millennial-scale features of atmospheric CH_4 over the past 800,000 years, Nature, 453, 383-386, 2008.

Lyon, B., and Barnston, A. G.: ENSO and the spatial extent of interannual precipitation extremes in tropical land areas, J. Clim., 18, 5095-5109, 2005.

MacDonald, G. M., Beilman, D. W., Kremenetski, K. V., Sheng, Y., Smith, L. C., and Velichko, A. A.: Rapid early development of circumarctic peatlands and atmospheric CH_4 and CO_2 variations, Science, 314, 285-288, 2006.

MacFarling-Meure, C., Etheridge, D., Trudinger, C., Steele, P., Langenfelds, R., van Ommen, T., Smith, A., and Elkins, J.: Law Dome CO_2, CH_4 and N_2O ice core records extended to 2000 years BP, Geophys. Res. Lett., 33, L14810, 2006.

Marchitto, T. M., Muscheler, R., Ortiz, J. D., Carriquiry, J. D., and van Geen, A.: Dynamical response of the tropical Pacific Ocean to solar forcing during the early Holocene, Science, 330, 1378-1381, 2010.

Marcott, S. A., Shakun, J. D., Clark, P. U., and Mix, A. C.: A reconstruction of regional and global temperature for the past 11300 years, Science, 339, 1198-1201, 2013.

Mischler, J. A., Sowers, T. A., Alley, R. B., Battle, M., McConnell, J. R., Mitchell, L., Popp, T., Sofen, E., and Spencer, M. K.: Carbon and hydrogen isotopic composition of methane over the last 1000 years, Global Biogeochem. Cycles, 23, GB4024, 2009.

Mitchell, L. E., Brook, E. J., Sowers, T., McConnell, J. R., and Taylor, K.: Multidecadal variability of atmospheric methane, 1000–1800 C.E., J. Geophys. Res., 116, G02007, 2011.

Mitchell, L. E., Brook, E. J., Lee, J. E., Buizert, C., and Sowers, T.: Constraints on the Late Holocene anthropogenic contribution to the atmospheric methane budget, Science, 342, 964-966, 2013.

Moy, C.M., Seltzer, G. O., Rodbell, D. T., and Anderson, D. M.: Variability of El Niño/Southern Oscillation activity at millennial timescales during the Holocene epoch, Nature, 420, 162-165, 2002.

Neff, U., Burns, S. J., Mangini, A., Mudelsee, M., Fleitmann, D., and Matter, A.: Strong coherence between solar variability and the monsoon in Oman between 9 and 6 kyr ago, Nature, 411, 290-293 2001.

Petrenko, V. V., Smith, A. M., Brook, E. J., Lowe, D., Riedel, K., Brailsford, G., Hua, Q., Schaefer, H., Reeh, N., Weiss, R. F., Etheridge, D., and Severinghaus, J. P.: 14CH4 measurements in Greenland ice: investigating last glacial termination CH_4 sources, Science, 324, 506-508, 2009.

Prather, M. J., Holmes, C. D., and Hsu, J.: Reactive greenhouse gas scenarios: Systematic exploration of uncertainties and the role of atmospheric chemistry, Geophys. Res. Lett., 39, L0980, 2012.

Rasmussen, S. O., Andersen, K. K., Svensson, A. M., Steffensen, J. P., Vinther, B. M., Clausen, H. B., Siggaard-Andersen, M. -L., Johnsen, S. J., Larsen, L. B., Dahl-Jensen, D., Bigler, M., Rothlisberger, R., Fischer, H., Goto-Azuma, K., Hansson, M. E., and Ruth, U.: A new Greenland ice core chronology for the last glacial termination, J. Geophys. Res., 111, D06102, 2006.

Renssen, H., Goosse, H., and Muscheler, R.: Coupled climate model simulation of Holocene cooling events: oceanic feedback amplifies solar forcing, Clim. Past, 2, 79-90, 2006.

Rhee, T. S., Kettle, A. J., and Andreae, M. O.: Methane and nitrous oxide emissions from the ocean: A reassessment using basin-wide observations in the Atlantic, J. Geophys. Res., 114, D12304, 2009.

Rhodes, R. H., Brook, E. J., Chiang, J. C. H., Blunier, T., Maselli, O. J., McConnell, J. R., Romanini, D., and Severinghaus, J. P.: Enhanced tropical methane production in response to iceberg discharge in the North Atlantic, Science, 348, 1016-1019, 2015.

Ruddiman, W. F., Kutzbach, J. E., and Vavrus, S. J.: Can natural or anthropogenic explanations of late-Holocene CO_2 and CH_4 increases be falsified?, The Holocene, 21, 865-879, 2011.Sanderson, M. G.: Biomass of termites and their emissions of methane and carbon dioxide: A global database, Global Biogeochem. Cy., 10, 543-558, 1996.

Sapart, C. J., Monteil, G., Prokopiou, M., van de Wal, R. S. W., Kaplan, J. O., Sperlich, P., Krumhardt, K. M., van der Veen, C., Houweling, S., Krol, M. C., Blunier, T., Sowers, T., Martinerie, P., Witrant, E., Dahl-Jensen, D., and Röckmann, T.: Natural and anthropogenic variations in methane sources during the past two millennia, Nature, 490, 85-88, 2012.

Schuur, E. A. G., McGuire, A. D., Schadel, C., Grosse, G., Harden, J. W., Hayes, D. J., Hugelius, G., Koven, C. D., Kuhry, P., Lawrence, D. M., Natali, S. M., Olefeldt, D., Romanovsky, V. E., Schaefer, K., Turetsky, M. R., Treat, C. C., and Vonk, J. E.: Climate change and the permafrost carbon feedback, Nature, 520, 171-179.

Severinghaus, J. P., Beaudette, R., Headly, M. A., Taylor, K., and Brook, E. J.: Oxygen-18 of O_2 records the impact of abrupt climate change on the terrestrial biosphere, Science, 324, 1431-1434, 2009.

Singarayer, J. S., Valdes, P. J., Friedlingstein, P., Nelson, S., and Beerling, D. J.: Late Holocene methane rise caused by orbitally controlled increase in tropical sources, Nature, 470, 82-86, 2011.

Sowers, T.: Atmospheric methane isotope records covering the Holocene period, Quat. Sci. Rev., 29, 213-221,2010.

Spahni, R., Schwander, J., Flückiger, J., Stauffer, B., Chappellaz, J. and Raynaud, D.: The attenuation of fast atmospheric CH_4 variations recorded in polar ice cores, Geophys. Res. Lett., 30, 1571, 2003.

Spahni, R., Chappellaz, J., Stocker, T. F., Loulergue, L., Hausammann, G., Kawamura, K., Flückiger, J., Schwander, J., Raynaud, D., Masson-Delmotte, V., and Jouzel, J.: Atmospheric methane and nitrous oxide of late Pleistocene from Antarctic ice cores, Science, 310, 1317-1321, 2005.

Sperlich, P., Schaefer, H., Mikaloff Fletcher, S. E., Guillevic, M., Lassey, K., Sapart, C. J., Röckmann, T., and Blunier, T.: Carbon isotope ratios suggest no additional methane from boreal wetlands during the rapid Greenland Interstadial 21.2, Global Biogeochem. Cycles, 29, 1962-1976, 2015.

Stocker, T. F., Qin, D., Plattner, G.-K., Tignor, M., Allen, S. K., Boschung, J., Nauels, A., Xia, Y., Bex, V., and Midgley, P. M. (Eds.): IPCC, 2013: Climate Change 2013: The Physical Science Basis, Contribution of Working Group I to the Fifth Assessment Report of the Intergovernmental Panel on Climate Change, Cambridge University Press, Cambridge, United Kingdom and New York, NY, USA, 1535 pp., 2013.

Taylor, K. C., Alley, R. B., Meese, D. A., Spencer, M. K., Brook, E. J., Dunbar, N. W., Finkel, R. C., Gow, A. J., Kurbatov, A. V., Lamorey, G. W., Mayewski, P. A., Meyerson, E. A., Nishiizumi, K., and Zielinski, G. A.: Dating the Siple Dome (Antarctica) ice core by manual and computer interpretation of annual layering, J. Glaciol., 50, 453-461, 2004.

Tzedakis, P. C., Pälike, H., Roucoux, K. H., and de Abreu, L.: Atmospheric methane, southern European vegetation and low-mid latitude links on orbital and millennial timescales, Earth Planet. Sci. Lett., 277, 307-317, 2009.

Valdes, P. J., Beerling, D. J., and Johnson, C. E.: The ice age methane budget, Geophys. Res. Lett., 32, L02704, 2005.

Wang, Y., Cheng, H., Edwards, R. L., He, Y., Kong, X., An, Z., Wu, J., Kelly, M. J., Dykoski, C. A., and Li, X.: The Holocene Asian monsoon: links to solar changes and north Atlantic climate, Science, 308, 854-857, 2005.

WAIS Divide Project Members: Precise interpolar phasing of abrupt climate change during the last ice age, Nature, 520, 661-665, 2015.

Walter, K. M., Zimov, S. A., Chanton, J. P., Verbyla, D., and Chapin III, F. S.: Methane bubbling from Siberian thaw lakes as a positive feedback to climate warming, Nature, 443, 71-75, 2006.

Walter, K. M., Edwards, M. E., Grosse, G., Zimov, S. A., and Chapin III, F. S.: Thermokarst lakes as a source of atmospheric CH_4 during the last deglaciation, Science, 318, 633-636, 2007.

Walter Anthony, K. M., Zimov, S. A., Grosse, G., Jones, M. C., Anthony, P. M., Chapin III, F. S., Finlay, J. C., Mack, M. C., Davydov, S., Frenzel, P., and Frolking, S.: A shift of thermokarst lakes from carbon sources to sinks during the Holocene epoch, Nature, 511, 452-456, 2014.

Weber, S. L., Drury, A. J., Toonen, W. H. J., and van Weele, M.: Wetland methane emissions during the Last Glacial Maximum estimated from PMIP2 simulations: Climate, vegetation, and geographic controls, J. Geophys. Res., 115, D06111, 2010.

Yu, Z., Loisel, J., Turetsky, M. R., Cai, S., Zhao, Y., Frolking, S., MacDonald, G. M., and Bubier, J. L.: Evidence for elevated emissions from high-latitude wetlands contributing to high atmospheric CH4 concentration in the early Holocene, Global Biogeochem. Cycles, 27, 1-10, 2013.

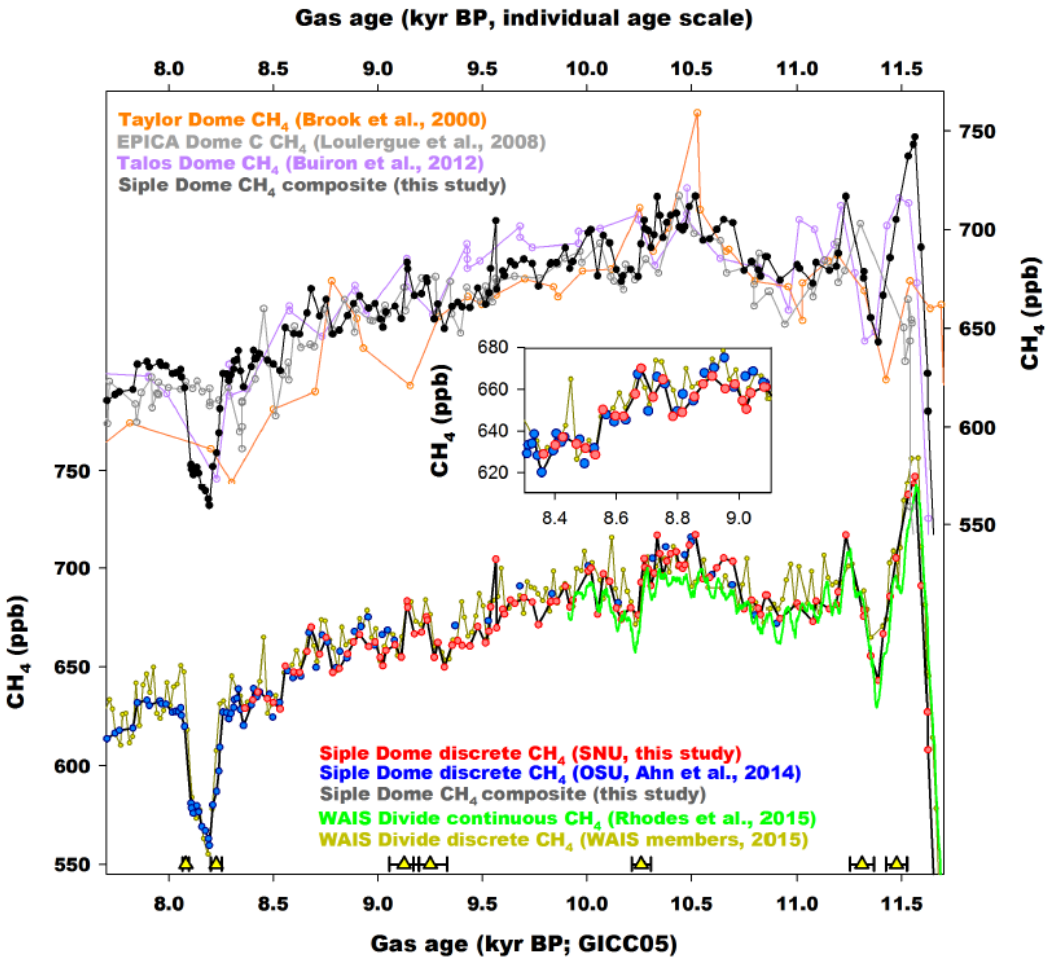

Figure 1. Atmospheric CH_4 concentration reconstructions during the early Holocene. Top: new high-resolution Siple Dome composite (black, this study and Ahn et al., 2014) compared with previous records from Taylor Dome (orange, Brook et al., 2000), EPICA Dome C (grey, Loulergue et al., 2008), and Talos Dome (purple, Buiron et al., 2012). Bottom: Siple Dome CH_4 records measured in OSU (blue, Ahn et al., 2014) and SNU (red, this study). Siple Dome composite (black line) is plotted with WAIS Divide discrete (dark yellow, WAIS Divide project members, 2015) and continuous measurement records (green, Rhodes et al., 2015). Inset: Enlarged plot showing overlapped interval between OSU and SNU Siple Dome data.

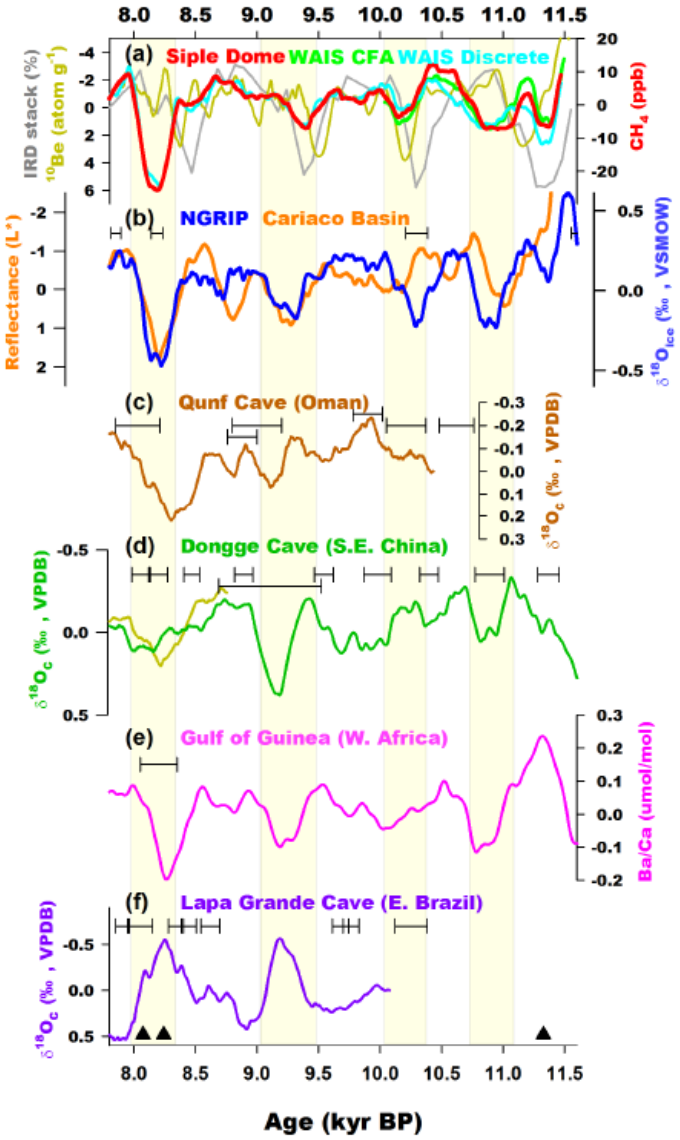

Figure 2. Millennial scale climate variability. All proxies present here were smoothed by 250-year running average and detrended by high-pass filter with 1/1800-year window. (a) Siple Dome CH_4 (red, this study), Greenland ^{10}Be (dark yellow, Finkel and Nishizumii, 1997), North Atlantic IRD stack (grey, Bond et al., 2001). Also shown are WAIS Divide CH_4 data by discrete (cyan, denoted "WAIS Discrete", WAIS Divide project members, 2015) and continuous (yellow green, denoted "WAIS CFA", Rhodes et al., 2015) technique. (b) NGRIP stable water isotope ratio (blue, Rasmussen et al., 2006) and Cariaco Basin reflectance (orange, Deplazes et al., 2013). (c) Qunf Cave speleothem oxygen isotope (Fleitmann et al., 2007). (d) Dongge Cave speleothem oxygen isotope (green, Dykoski et al., 2005; dark yellow, Wang et al., 2005). (e) Gulf of Guinea planktonic Ba/Ca ratio (Weldeab et al., 2007). (f) Lapa Grande Cave speleothem oxygen isotope (purple, Strikis et al., 2011). Black solid triangles are age tie-points used to adjust Siple Dome and WAIS Divide CH_4 data to GICC05 scale.

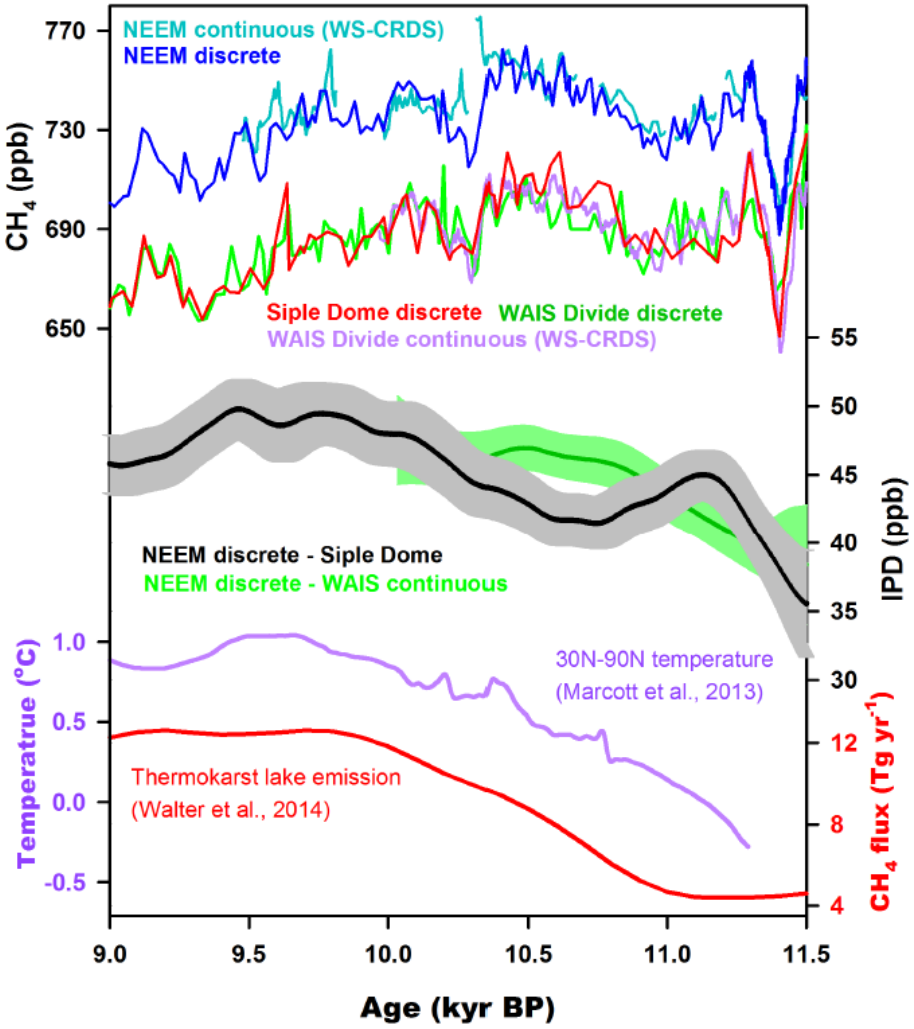

Figure 3. CH_4 inter-polar difference (IPD) and high latitude CH_4 sources. Top: High resolution CH_4 discrete measurements from NEEM discrete (blue, Chappellaz et al., 2013), NEEM continuous (turquoise, Chappellaz et al., 2013), WAIS Divide discrete (yellow green, WAIS Divide project members, 2015), WAIS Divide continuous (purple, Rhodes et al., 2015), and Siple Dome (red, this study) ice core records. Middle: 1000-year low-pass filtered IPD-1 (black) and IPD-2 (green) with 95 % significance interval (shaded). Bottom: Proxy-based temperature reconstruction for 30°N-90°N and 30°S-30°N latitude (blue, Marcott et al., 2013). CH_4 flux estimate from Siberian- and Alaskan thermokarst lakes (red, Walter-Anthony et al., 2014).

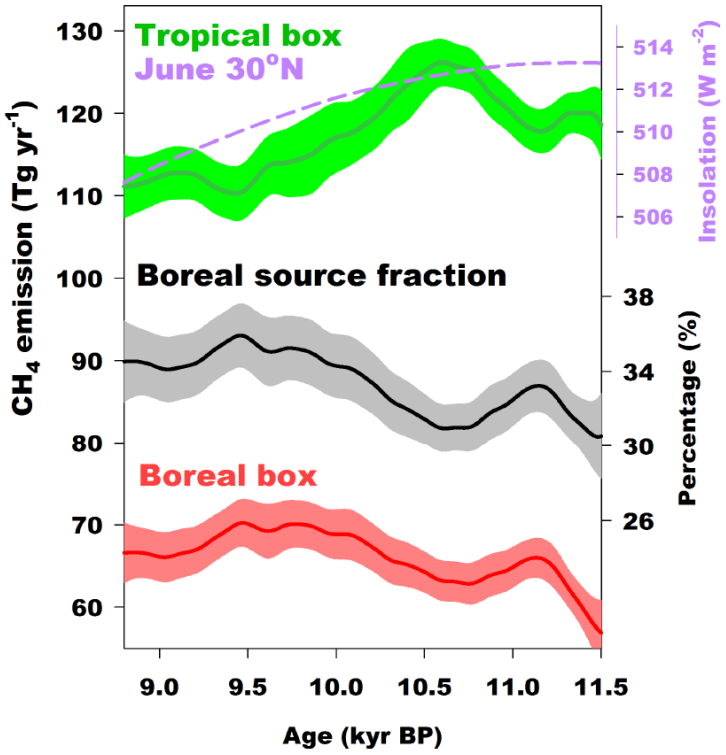

Figure4. 3-box source distribution model results of tropical (green) and boreal (red) boxes. Black line shows the boreal to total source fraction (see text). Purple dashed line plotted with tropical emission is summer insolation in 30°N (Berger and Loutre, 1991).

5

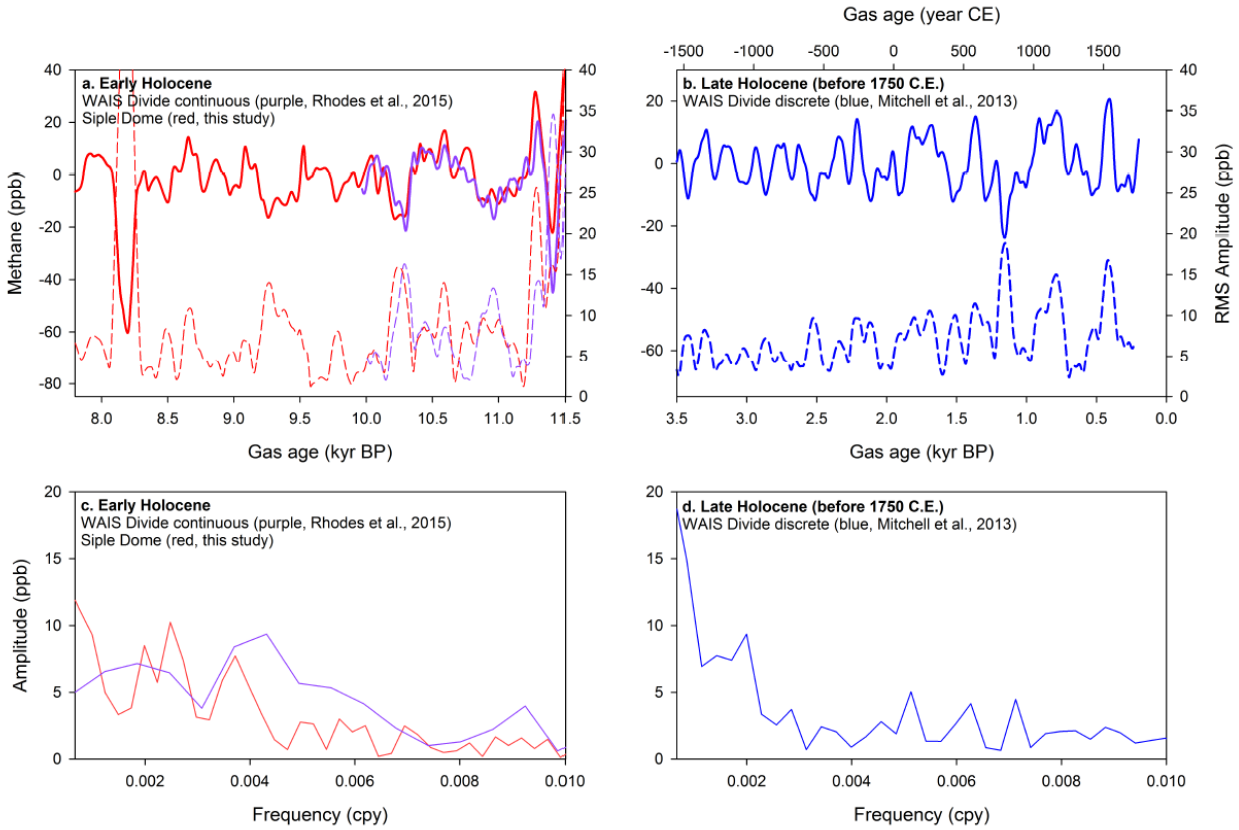

Figure 5. Upper: Detrended (75 to 1800-year band-pass filtered) CH_4 for the early (a) and late (b) Holocene from Siple Dome (red, this study), WAIS divide continuous (purple, Rhodes et al., 2015), and WAIS divide discrete (blue, Mitchell et al., 2013) data. Dashed lines are root mean square (RMS) amplitude running averaged by 75-year window. Lower: Amplitude spectrum of Early (c) and Late (d) Holocene CH4 records. Note that CH_4 data before 1750 C.E. are used for the preindustrial late Holocene.

Table 1. 3-box source distribution model results of tropical (green, T) and boreal (red, N) boxes and boreal source fraction (N/(T+N+S)) compared with previous results. Errors denote 95% confidence interval.

Ref.	N box	T box	Boreal source fraction N/(N+T+S)
(ka)	($Tg\ yr^{-1}$)		(%)
Brook et al., 2000 (9.5-11.5 ka)	64 ± 5	123 ± 8	32 ± 3
Chappellaz et al., 1997 (9.5-11.5 ka)	66 ± 8	120 ± 9	33 ±3
This study (9.5-11.5 ka)	66 ± 4	120 ± 4	33 ± 2
This study (11.5 ka)	47 ± 9	149 ± 10	22 ± 5
This study (9.9 ka)	65 ± 8	119 ± 9	33 ± 5